Journal of Chromatography, 557 (1991) 369–382
Elsevier Science Publishers B.V., Amsterdam

CHROM. 23 308

Adsorption–desorption isotherm hysteresis of β-lactoglobulin A with a weakly hydrophobic surface

SHIWEN LIN, RIGOBERTO BLANCO and BARRY L. KARGER*
Barnett Institute, Northeastern University, Boston, MA 02115 (USA)

ABSTRACT

Adsorption–desorption isotherms of bovine β-lactoglobulin A (β-lact A) on a weakly hydrophobic stationary phase (C_1-ether) were measured by frontal analysis. The adsorption isotherms obtained at different pH were found to be dramatically different in shape, column capacity and desorption reversibility. At pH 4.5, an S-shaped adsorption isotherm was observed whereas at pH 6.0 a Langmuir isotherm was found. In addition, the desorption isotherm at pH 6.0 was found to overlap with the adsorption isotherm, and the adsorption–desorption process of β-lact A under this condition could be characterized by a fully reversible Langmuir model. The desorption isotherm at pH 4.5, however, did not retrace the adsorption isotherm, resulting in hysteresis loops. A higher aggregate (tetramer) of β-lact A is shown to be in an equilibrium with the β-lact A protomer (dimer) at pH 4.5 whereas the dimer alone is predominant at pH 6.0. It is further shown that changes in the adsorption coefficient between the adsorption and the desorption cycles for the tetramer at pH 4.5 can account for the hysteresis. The results demonstrate that pH can be a sensitive parameter in protein adsorption isotherm behavior and ultimately the behavior of species in preparative-scale chromatography.

INTRODUCTION

The investigation of protein adsorption at liquid–solid interfaces is of great importance in many fields, including the chromatographic separation of proteins and the design of biomaterials and biosensors [1–3]. The measurement of the adsorption isotherm can provide important information on the adsorption process: for example, adsorption isotherms can be used as a tool in the prediction of elution behavior in the preparative-scale chromatography of proteins [4]. In preparative-scale liquid chromatography, loading of relatively high concentrations of substances is a common practice, and protein–protein interaction leading to association or aggregation can be an important consideration at such high concentrations [5]. Multiple equilibria between oligomers open up a new dimension of complexity in such systems, and significant effects on adsorption behavior can be expected [6]. An understanding and control of such behavior can be important in chromatography, as well as in general protein adsorption phenomena.

β-Lactoglobulin A (β-lact A) is a classical example of a protein aggregating system, in which self-association can occur to different extents, depending on the pH

0021-9673/91/$03.50

and other conditions of the system [7]. Below pH 3.5, the dimeric β-lact A (molecular weight, MW 36 800) tends to dissociate to a nearly spherical monomer (MW 18 400). Between pH 3.7 and 5.2 (pI = 5.2), dimers can associate to form higher order aggregates, with the distribution depending on the total concentration and with a maximum extent of self-association occurring at pH 4.5 and 4°C [8]. Above pH 5.2, species larger than dimer decrease in relative amount and the stable dimeric form is predominant at pH 6.0 [7].

Previously, we have demonstrated the separation of three aggregated species of β-lact A, a tetramer, octamer and dodecamer, by hydrophobic interaction chromatography on a C_1-ether phase column with a gradient from 3 to 0 M ammonium sulfate (pH 4.5) at 4°C [5]. On the other hand, a single species was eluted at pH 6.0. More recently, we reported an S-shaped adsorption isotherm of β-lact A on the C_1-ether phase with 0.85 and 1.0 M ammonium sulfate at pH 4.5 [6]. The S-shaped isotherm was interpreted in terms of two species, a protomer and a higher order stronger adsorbing species in the stoichiometric ratio of 1:2, and an explicit adsorption isotherm equation was developed for the aggregating system. We also noted that adsorption hysteresis occurred in this system.

Although other hysteresis phenomena involving proteins, such as enzymatic activity hysteresis and thermal sol–gel hysteresis, have been known for decades, protein adsorption hysteresis has drawn increasing attention only recently [9]. Hysteresis is a characteristic phenomenon in protein adsorption where, for example, conformational or reorientational changes on the hydrophobic adsorbent surface (alkyl-derivatized agarose beads) can result in altered species which bind more strongly to the surface [9–11]. In addition, a recent study on the adsorption isotherm of albumin on a TSK-DEAE anion exchanger also pointed to a probable desorption hysteresis because of non-specific hydrophobic adsorption and possible conformational alerations leading to stronger binding [12].

In this paper, as a continuation of our previous work, both the adsorption and desorption isotherms of β-lact A on a weakly hydrophobic surface at pH 4.5 and 6.0 are examined in depth. Adsorption–desorption isotherms of β-lact A at pH 4.5 again revealed hysteresis loops, with an S-shaped adsorption isotherm and a series of Langmuir-shaped desorption isotherms. The behavior is shown to result from an increase in the adsorption coefficient of the aggregate in the desorption cycle relative to the adsorption cycle. At pH 6.0, on the other hand, both the adsorption and desorption isotherms were found to be Langmuirian in shape and fully reversible. The results point to the dramatic changes in adsorption–desorption behavior that can result when the mobile phase conditions are altered.

EXPERIMENTAL

Equipment

Fig. 1 depicts schematically the apparatus used for isotherm measurements. Frontal chromatography was conducted on a system consisting of an Altex 110A microflow pump with an Altex 420 system controller (Beckman, San Ramon, CA, USA), two Model 7125 syringe-loading sample injection valves (Rheodyne, Cotati, CA, USA) with two 1-ml loops, and a photodiode-array detector (Hewlett-Packard, Palo Alto, CA, USA). The photodiode-array detector was used specifically to mon-

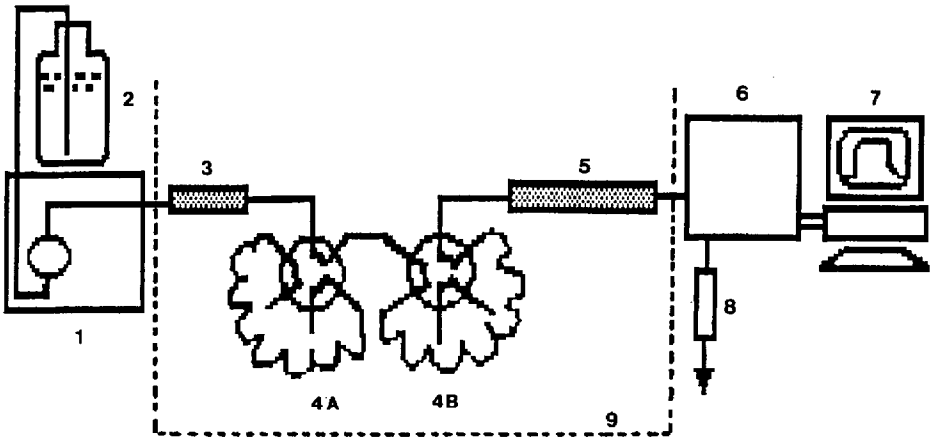

Fig. 1. Instrument for isotherm measurements. 1 = Pump; 2 = mobile phase reservoir; 3 = precolumn; 4A = loop A, 1 ml; 4B = loop B, 1 ml; 5 = analytical column; 6 = photodiode-array detector; 7 = workstation; 8 = flow-rate monitor; 9 = thermostated water-bath.

itor the UV spectra of the protein solute during the breakthrough curve and in the plateau region to search for any structural alteration of the protein in the frontal analysis [13]. The chromatograms and spectra were collected and stored in an HP 9000 workstation through HP 7996A operating software (Hewlett-Packard).

The column packing consisted of Vydac silica (Separation Group, Hesperia, CA, USA) bonded with a methyl polyether (C_1-ether) phase (particle size 5 μm, pore diameter 300 Å, specific surface area 72 m^2/g) and prepared as described elsewhere [14]. The surface coverage was 6.3 $\mu mol/m^2$, as determined by elemental analysis (assuming a bonding stoichometry of two ethoxy groups of the silane to silica). The 28 mm × 2.9 mm I.D. column was slurry packed under pressure in carbon tetrachloride–methanol (70:30, v/v) with methanol as driving solvent. The temperature of the column, sample loop and tubing connecting the pump to the injector was regulated at 5 ± 0.5°C by a thermostated water-bath (Neslab, Portsmouth, NH, USA).

Reagents

HPLC-grade water, analytical-reagent grade acetic acid and ammonia solution were purchased from J. T. Baker (Phillipsburg, NJ, USA). 4-(2-Hydroxyethyl)-1-piperazineethanesulfonic acid (HEPES) and 2-(N-morpholino)ethanesulfonic acid (MES) buffer were obtained from Research Organics (Cleveland, OH, USA). High-purity ammonium sulfate (treated to reduce the content of heavy metals) and electrophoretically pure bovine β-lactoglobulin A were purchased from Sigma (St. Louis, MO, USA).

Procedures

The mobile phase solutions were prepared by dissolving the correct weight of salt (0.85 *M* ammonium sulfate) and buffer (20 m*M* HEPES–20 m*M* MES–20 m*M* acetic acid) in HPLC water, adjusting the pH to 4.5 or 6.0 with either acetic acid or

ammonia solution, transferring the solution to a volumetric flask and diluting to volume with water. Mobile phase solutions were filtered and degassed under vacuum before use. Protein samples were freshly prepared in the mobile phase buffer and filtered through a 0.45-μm membrane immediately before each injection.

Adsorption isotherm determination

The column was first equilibrated with at least 100 column volumes of the mobile phase buffer, followed by loading of the protein solution through loop B (Fig. 1). At 23 min after the outlet UV absorbance of the eluent had reached a plateau in frontal development, the pure mobile phase buffer (*i.e.*, without protein dissolved) was switched into the column to elute the adsorbed protein and to regenerate the surface for the next loading. Protein concentration was monitored at 310 nm. Calibration graphs at this wavelength showed a linear relationship between the concentration used and the absorbance response. The adsorbed amount per unit volume of stationary phase (Q) equilibrated with a given concentration of protein in solution was derived from the breakthrough curve as follows:

$$Q = FA_a/\varepsilon V_s \tag{1}$$

where F is the flow-rate, A_a is the area of the retained portion of the breakthrough curve, as described previously [6], ε is the molar absorptivity in mAU ml/mg of β-lact A in the mobile phase buffer measured from the calibration graph at 310 nm and V_s is the volume of stationary phase determined by a standard weight difference method, using methanol and carbon tetrachloride [15,16].

The recovery derived from the ratio of the rear boundary area to the front boundary area after each elution with the pure mobile phase was 98 ± 3% (three runs). This means that each loading run began with a clean regenerated surface. The flow-rate was measured periodically at the detector outlet by using a buret and an electronic timer. The outlet flow-rate was determined to be constant (± 1 μl/min) during the injection of the sample, uptake of the protein and in the plateau region. The adsorbed amount was found to be constant within 5% over a 10-fold range of flow-rate (10, 20, 50 and 100 μl/min) for a given solution concentration of protein, indicating that the mass transfer inside and outside the pores of the adsorbent was rapid in the present system.

Desorption isotherm determination

Protein sample was first loaded into the column through loop B as above. Instead of switching to pure mobile phase buffer at 20 min, after a stable plateau had developed, a sample of lower concentration was introduced into the column through loop A to elute a portion of the adsorbed protein. Loop A was loaded with a lower concentration of sample and the valve was rotated to the injection position while loop B was still in the injection position. After the sample solution passed through the connecting tubing between the loops, loop B was switched back to the loading position to allow the lower concentration sample in loop A to pass onto the column. After a lower plateau had developed, the pure mobile phase buffer was switched into the column to elute the remainder of the adsorbed protein.

The desorption isotherms were constructed by using the adsorbed amount of protein on the stationary phase derived as follows:

$$Q(C) = Q_0(C_0) - \frac{F}{\varepsilon V_S} \cdot A_d \tag{2}$$

where $Q(C)$ is the amount of adsorbed protein on the stationary phase in mg/ml equilibrated with a solution concentration C, $Q_0(C_0)$ is the initial amount of adsorbed protein equilibrated with the solution concentration C_0 and A_d denotes the area in mAU min under each elution breakthrough curve (see Fig. 2). Each desorption was initiated from the same adsorbed state $Q(C_0)$. Two initial states (C_0 = 10.0 and 15.0 mg/ml) were used to obtained two separate desorption isotherms.

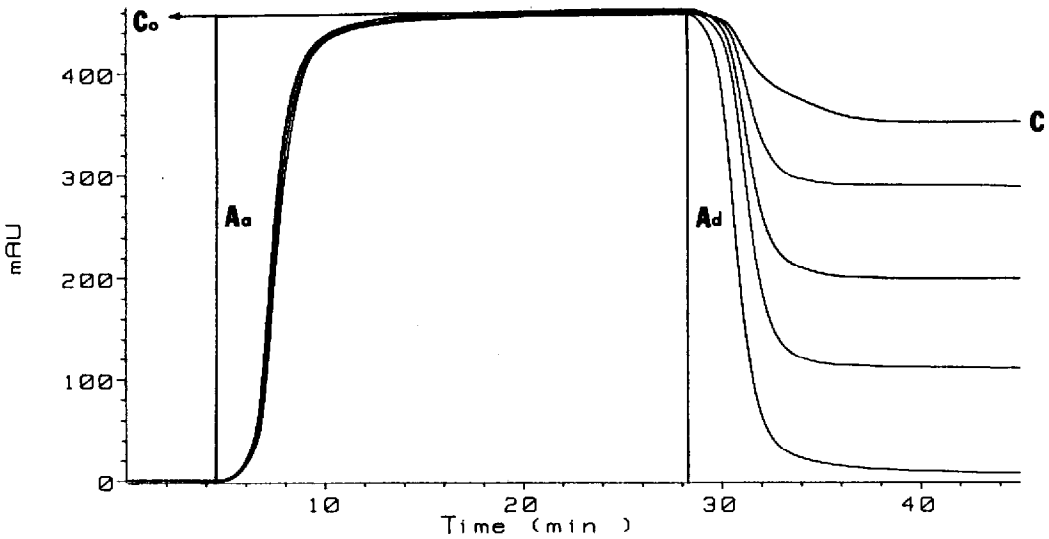

Fig. 2. Frontal chromatograms for the determination of the desorption isotherms. Column, C_1-ether (28 mm × 2.9 mm I.D.); sample, β-lact A in mobile phase buffer, 530-μl injection; mobile phase, 0.85 *M* ammonium sulfate–0.02 *M* HEPES–0.02 *M* MES–0.02 *M* acetic acid, pH adjusted to 4.5 or 6.0 with acetic acid or ammonia solution; flow-rate, 23.0 μl/min; pure mobile phase was switched into the column at 23 min; temperature, 5°C.

RESULTS AND DISCUSSION

Frontal analysis and elution chromatography

Frontal analysis breakthrough curves and slopes (first derivative) for β-lact A at pH 4.5 and 6.0 are shown in Fig. 3. At pH 4.5 both the front and rear boundaries appear more diffuse compared with those at pH 6.0, owing to the relatively shallow first-derivative trace. This is an unusual behavior because in general the front and rear boundaries are alternatively diffuse and self-sharpening, exhibiting either a Langmuir or an anti-Langmuir shape. The diffuse front and rear boundaries for the present system of β-lact A adsorption on the C_1-ether phase at pH 4.5 suggest changes in the

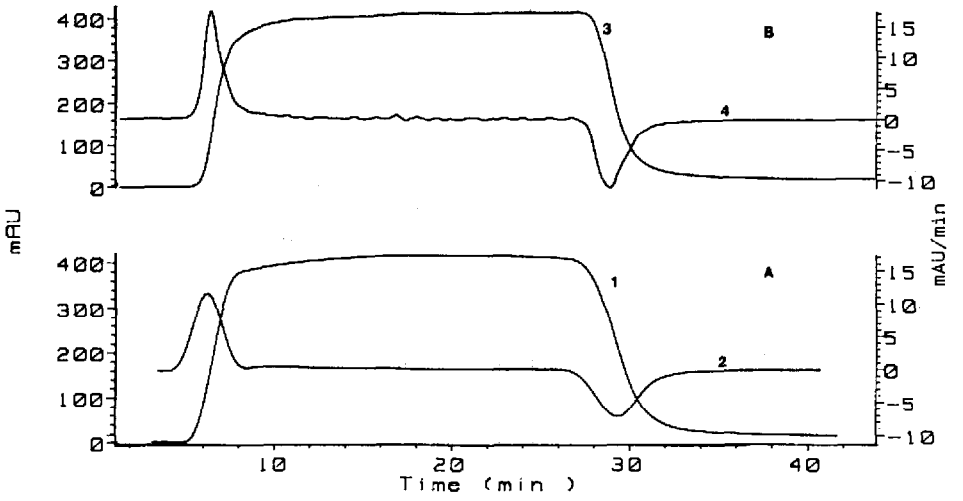

Fig. 3. Frontal chromatograms of β-lact A on the C_1-ether column at pH (A) 4.5 and (B) 6.0. Detection wavelength, 310 nm; curves 1 and 3, frontal chromatograms; curves 2 and 4, slope of frontal chromatograms. Other conditions as in Fig. 2.

adsorption–desorption process. At pH 6.0, on the other hand, the sharper front boundary compared with the rear boundary as identified by the derivative trace indicates a Langmuirian isotherm.

The broader band spreading at pH 4.5 relative to that at pH 6.0 can also be seen from the isocratic elution chromatograms in Fig. 4. The slightly longer retention of

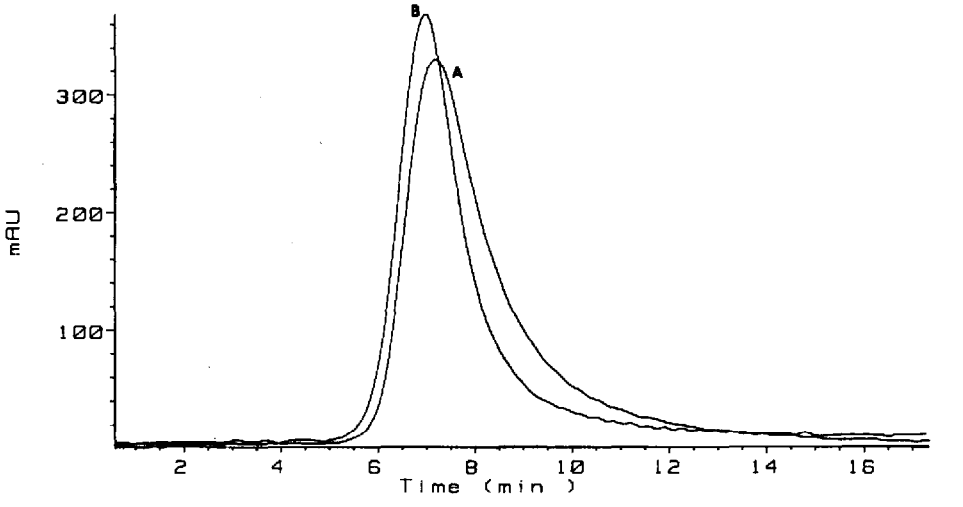

Fig. 4. Isocratic elution chromatograms of β-lact A on the C_1-ether column at pH (A) 4.5 and (B) 6.0. Conditions as in Fig. 2, except that 5.0 mg/ml of β-lact A in mobile phase buffer and 20 μl injections were used.

β-lact A at pH 4.5 indicated a stronger interaction. The band broadening may be a result of the presence of multiple species at pH 4.5 which co-elute under the present conditions [6], whereas these species could be resolved by other conditions [5].

The adsorbed amount of protein, Q, was determined from the retained portion of the breakthrough curves from eqn. 1. By definition, the adsorbed amount Q at equilibrium or at the steady state should be independent of the mobile phase flow-rate used for the measurements. Indeed, as already noted, Q was found to be constant within 5% over a tenfold range of flow-rate (10–100 μl/min), for a given solution concentration of protein.

The desorption isotherm was derived from the frontal analysis as depicted in Fig. 2. As already noted, each desorption step began with the same amount of adsorbed protein corresponding to a specific solution concentration $Q(C_0)$. After the elution with a protein solution of lower concentration, the amount of protein left in the stationary phase was derived from eqn. 2. These results were used to construct the desorption isotherm. The amount of desorbed protein during the elution experiments was also found to be independent of flow-rate in the range 10–100 μl/min.

The UV spectra during the frontal analysis were collected by the photodiode-array detector. As in the plateau region the absorbance at the maximum wavelength (280 nm) was not in the linear range of the detector, only the spectra taken at the beginning of the front boundary and at the end of the rear boundary were compared. No differences were found betweeen the normalized spectra or the second-derivative spectra, indicating no major unfolding of the protein during the adsorption and desorption processes. This result, however, does not exclude the association of β-lact A during the frontal analysis, as the UV spectra for different oligomers are similar [6].

Adsorption–desorption isotherms

In principle, binding equilibria of a solute to an adsorbent from a liquid phase can be obtained by either adsorption or desorption. In a thermodynamically reversible system, the equilibria obtained by the two procedures will be identical, *i.e.*, the adsorption isotherm will be retraced by the desorption isotherm. This is the case for the adsorption of β-lact A at pH 6.0 on the C_1-ether phase.

At pH 6.0, the Langmuir adsorption and desorption isotherms of β-lact A on the C_1-ether phase overlap each other, as shown in Fig. 5. This result suggests full reversibility in the adsorption and desorption steps. In addition, a linear relationship ($r^2 = 0.990$) of Q/C *vs.* Q was observed in the Scatchard plot for the isotherms at pH 6.0, as shown in the inset in Fig. 5. The adsorption–desorption process at pH 6.0 can thus be characterized by the Langmuir model (*i.e.*, single species, uniform adsorption site, no lateral interaction or association on the surface). This result can be easily understood, as β-lact A in solution at pH 6.0 is a stable dimeric species (MW 36 800) [7]. Our previous gradient chromatographic results on the C_1-ether phase column [5] also demonstrated that β-lact A exists as a single species on the C_1-ether phase surface at pH 6.0 during the chromatographic process.

In contrast, at pH 4.5 the adsorption isotherm of β-lact A on the C_1-ether phase was not retraced by the desorption isotherm, resulting in hysteresis. Fig. 6 depicts the adsorption and desorption isotherms and the hysteresis loops at pH 4.5. As previously, an S-shaped isotherm [6] was obtained for the adsorption (or loading) process. The

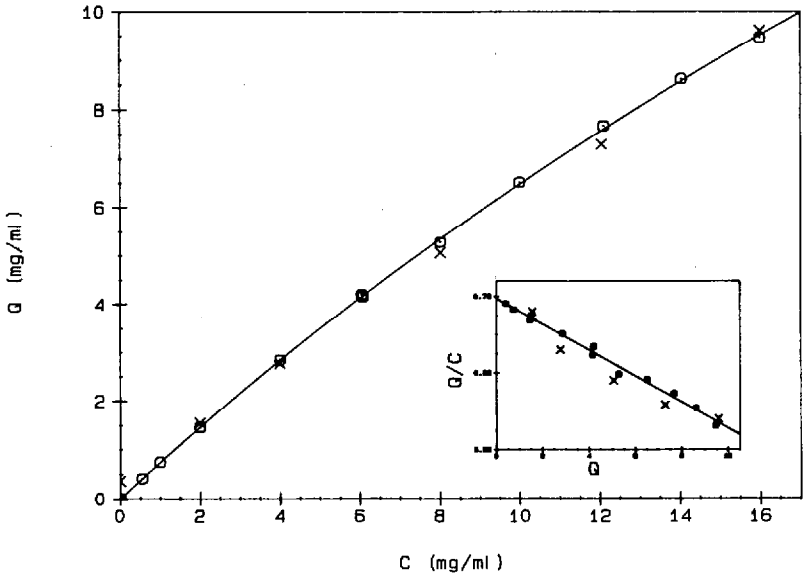

Fig. 5. Adsorption–desorption isotherm of β-lact A on C_1-ether phase at pH 6.0. (○) Adsorption; (×) desorption. Inset: Scatchard plot of the adsorption–desorption isotherm.

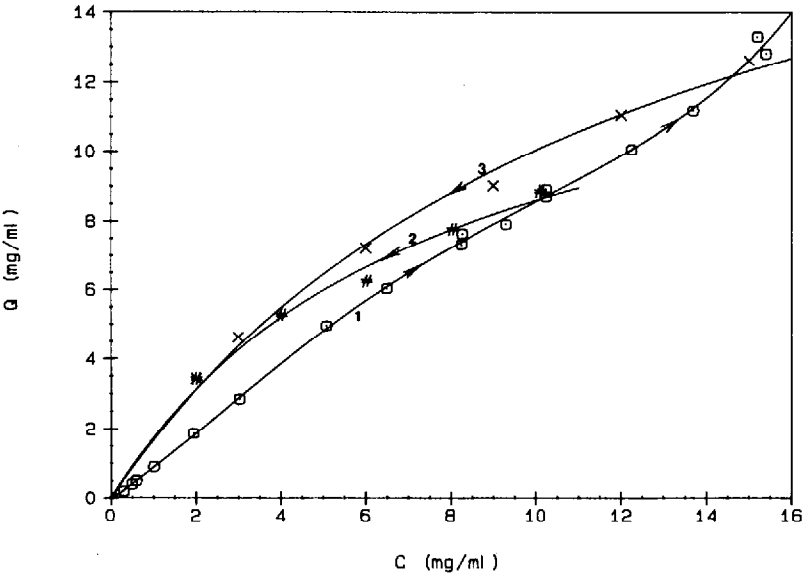

Fig. 6. Adsorption–desorption isotherms of β-lact A on C_1-ether phase at pH 4.5 (1) Adsorption isotherm; (2) desorption isotherm from 15.0 mg/ml of β-lact A equilibrated stationary phase; (3) desorption isotherm from 10.0 mg/ml of β-lact A equilibrated stationary phase. Other conditions as in Fig. 2.

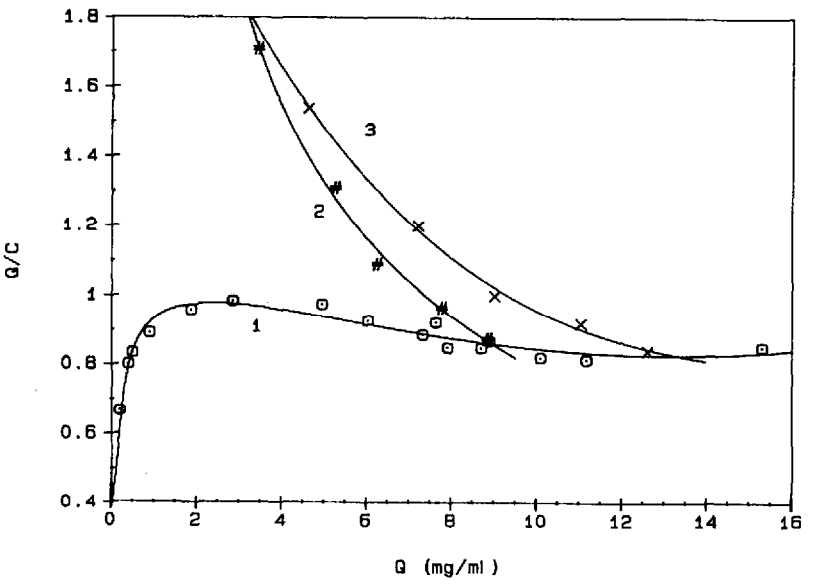

Fig. 7. Scatchard plots of the adsorption–desorption isotherms of β-lact A on the C_1-ether phase at pH 4.5. Conditions as in Fig. 2.

S-shape is indicative of positive cooperativity of protein adsorbate in which either association between molecules in solution [6] or lateral interaction or association between the adsorbed molecules on the surface can occur. The desorption isotherms, however, are Langmuir shaped. These isotherms form closed loops which can only be traced in one direction (see arrows in Fig. 6) as imposed by adsorption or desorption, respectively, The size of the hysteresis loop depends on the original amount of adsorbed protein. Changes in affinity and the shape of the isotherm between the adsorption and desorption branch indicate a change in the adsorbed state of the protein from the loading to the desorption steps.

The Scatchard plot is one of the most widely used methods to obtain a macroscopic indication of the type of cooperativity in the binding reaction. Fig. 7 presents Scatchard plots derived from the adsorption and desorption isotherms. A positive initial slope, characteristic of positive cooperativity in the low protein concentration region, was obtained for the adsorption process, while convex downwards Scatchard plots were observed for the desorption isotherms. Such convex downwards Scatchard plots reveal negative cooperativity in the process represented by the desorption isotherm.

Model for adsorption–desorption hysteresis

Positive cooperativity in the adsorption isotherm at low protein concentration has been previously interpreted in terms of the association of β-lact A protomer (A) in solution to form a stronger adsorbing oligomer (B) with a stoichiometry of two [6]:

$$2A \overset{K_e}{\rightleftharpoons} B \qquad [B] = K_e[A]^2 \tag{3}$$

$$A + mS \underset{k_{-a}}{\overset{k_a}{\rightleftharpoons}} AS_m \tag{4}$$

$$B + nS \underset{k_{-b}}{\overset{k_b}{\rightleftharpoons}} BS_n \tag{5}$$

where K_e is the apparent association equilibrium constant (l/mol) in solution from A to B, S is the available C_1-ether ligand concentration on the surface, k_a and k_{-a} are adsorption and desorption rate constants for the protomer A, respectively, k_b and k_{-b} are adsorption and desorption rate constants for the oligomer B, respectively, and m and n are the number of interaction sites between the surface and the protomer and oligomer, respectively.

Using low-angle laser light scattering (LALLS) [17], we found that under the same buffer conditions as in the isotherm measurement, at pH 4.5 and 5°C, a low concentration (< 1.0 mg/ml) of β-lact A appeared as the dimeric form (experimental MW $\approx$33 000). In the concentration range 1.0–10.0 mg/ml, the scattering function [17] could not be extrapolated to give an exact molecular weight because of changes in the relative amounts of two species in the association equilibrium with protein concentration. As the association was well characterized by a stoichiometry of two [6], it is reasonable to assume that an equilibrium between dimer and tetramer exists in this protein concentration range. Hence the above-discussed protomer represents the dimer (MW 36 800) and the oligomer represents the tetramer (MW 73 600).

According to the rate law, the adsorption rate of the dimer and tetramer can be expressed as

$$dq_A/dt = k_a C_A[S]^m - k_{-a}q_A \tag{6}$$

$$dq_B/dt = k_b C_B[S]^n - k_{-b}q_B \tag{7}$$

where q_A and q_B are the adsorbed concentrations of dimer $[AS_m]$ and tetramer $[BS_n]$ in mg/ml, respectively, and C_A and C_B are the solution concentrations of the dimer A and tetramer B, respectively. At steady state, $dq_A/dt = dq_B/dt = 0$, and eqns. 6 and 7 can be rearranged to

$$q_A = [S]^m(k_a/k_{-a})C_A \tag{8}$$

$$q_B = [S]^n(k_b/k_{-b})C_B \tag{9}$$

Assuming a constant surface availability ($[S] = [S_0]$ = constant) during adsorption in the low concentration region, as applied by Lapidus and Amundson [18] and Golshan-Shirazi and Guiochon [19], we can obtain

$$Q = q_A + q_B = [S]^m(k_a/k_{-a})C_A + [S]^n(k_b/k_{-b})C_B \tag{10}$$

$$Q = K_A C_A + K_B C_B \tag{11}$$

where

$$K_A = [S_0]^m(k_a/k_{-a}) \tag{12}$$

$$K_B = [S_0]^n(k_b/k_{-b}) \tag{13}$$

and K_A and K_B are the apparent adsorption coefficients of dimer A and tetramer B, respectively. From the expression of the solution association constant and total concentration, C, C_A and C_B can be derived as follows:

$$C_B = K_e^* C_A^2 \tag{14}$$

$$C = C_A + C_B \tag{15}$$

where K_e^* is the apparent association constant (ml/mg) in solution from dimer to tetramer when C_A and C_B are in the units of mg/ml. From the model of the stoichiometry of dimer to tetramer, we can derive that

$$C_A = [(1 + 4K_e^*C)^{1/2} - 1]/2K_e^* \tag{16}$$

$$C_B = C - [(1 + 4K_e^*C)^{1/2} - 1]/2K_e^* \tag{17}$$

By substituting eqns. 16 and 17 into eqn. 11, we can obtain an explicit expression for the adsorption isotherm of this aggregating system:

$$Q = K_BC - (K_B - K_A)[(1 + 4K_e^*C)^{1/2} - 1]/2K_e^* \tag{18}$$

This is the same expression as that rearranged from eqn. 17 in ref. 6, except that a factor of 2 has been included in K_e^*. Fitting the experimental data to the isotherm equation and corresponding Scatchard plots, values of $1.8 \cdot 10^4$ ml/mg, 0.34 and 1.2 were obtained for K_e^*, K_A and K_B, respectively.

The desorption rate in an elution process of dimer and tetramer can be expressed as

$$-dq_A/dt = k_{-a}q_A - k_aC_A[S_0]^m(1 - Q/Q_{max}) \tag{19}$$

$$-dq_B/dt = k_{-b}q_B - k_bC_B[S_0]^n(1 - Q/Q_{max}) \tag{20}$$

assuming a saturation capacity Q_{max} for each of the desorption isotherm, Q/Q_{max} is the fractional surface coverage and $(1 - Q/Q_{max})$ represents the availability of the ligand for readsorption. At steady state, $-dq_A/dt = -dq_B/dt = 0$, and substituting eqns. 12 and 13 into eqns. 19 and 20, we obtain

$$q_A = K_AC_A(1 - Q/Q_{max}) \tag{21}$$

$$q_B = K_BC_B(1 - Q/Q_{max}) \tag{22}$$

and

$$Q = \frac{K_A C_A + K_B C_B}{1 + (K_A C_A + K_B C_B)/Q_{max}} \tag{23}$$

By substituting eqns. 16 and 17 into eqn. 23, the desorption isotherm can be expressed as

$$Q = \frac{K_B C - (K_B - K_A)[(1 + 4K_e^* C)^{1/2} - 1]/2K_e^*}{1 + (1/Q_{max})\{K_B C - (K_B - K_A)[(1 + 4K_e^* C)^{1/2} - 1]/2K_e^*\}} \tag{24}$$

Fitting the experimental data in Fig. 6 for the desorption isotherm at pH 4.5 according to the above equation and assuming the value of $1.8 \cdot 10^4$ ml/mg for K_e^*, the apparent adsorption coefficients K_A and K_B for the dimer and tetramer, respectively, during the elution branch of the hysteresis loop can be obtained. The results are given in Table I.

Interestingly, from the adsorption branch to the desorption side of the isotherm a 1.5-fold increase in the adsorption coefficient for the tetramer (K_B) was observed, while the binding constant for the dimer (K_A) remained constant. In addition, K_B for the desorption branches was found to be the same, within experimental error, independent of the adsorption–desorption loop. This result suggests that the increase in K_B from the adsorption branch to the desorption branch is characteristic of the system, as fundamentally an infinite number of loops can be obtained over the whole concentration range. It can thus be seen that the existence of hysteresis is accompanied by the formation of adsorbing species with a significant increase in the apparent adsorption coefficient, as found by others [11].

The increase in the apparent adsorption coefficient for the tetramer may be a consequence of reorientation, *e.g.*, from head-on to side-on or from edge-on to face-on. Based on X-ray scattering results Timasheff and co-workers [20,21] proposed a tetramer sturcture for β-lact A in which the four subunits lie in a distorted plane to form a non-spherical, asymmetric structure. Thus, the accommodation of the adsorbed tetramer from an edge-on to a face-on state on the hydrophobic surface could

TABLE I

PARAMETERS DERIVED FROM ISOTHERM CURVE FITTING

pH	Isotherm branch	Adsorption coefficient	
		Dimer	Tetramer
4.5	Adsorption	0.34	1.2
	Desorption, $C = 15.0 \rightarrow 0$, $Q = 12.6 \rightarrow 0$	0.34	1.9
	Desorption, $C = 10.0 \rightarrow 0$, $Q = 8.85 \rightarrow 0$	0.34	1.8
6.0	Adsorption	0.76[a]	–
	Desorption	0.76[a]	–

[a] Langmuir constant *a*, *i.e.* binding constant for the single species at pH 6.0.

occur with a relatively stronger interaction with the surface after reorientation. It should also be noted that there is no evidence to rule out the possibility of a conformational change on the surface. However, the on-line UV spectra and second-derivative spectra collected during the adsorption and desorption (see earlier) indicate that a major conformational change on the surface is less likely. The constant adsorption coefficient for the dimer, K_A, from the adsorption and desorption branches also points to unlikely unfolding. The larger size and the asymmetric shape of the tetramer may result in different strength upon reorientation on the surface.

CONCLUSIONS

This study has demonstrated the role of protein association on the adsorption of β-lactoglobulin A on a weakly hydrophobic surface. The observed hysteresis in the adsorption and desorption cycles has been analyzed in terms of an increase in the binding of the tetramer while in contact with the surface. Although a conformational change of the tetramer on the surface cannot be ruled out, the asymmetric shape and size of this species make it more likely that a surface reorientation has taken place. If this is so, the reorientation presumably leads to the stronger binding.

It is most interesting that a change in pH of the solution leads to a dramatic change in isotherm behavior. This result is a direct consequence of the significantly reduced tendency of β-lactoglobulin A to protein association at pH 6.0, relative to pH 4.5. A possible strategy for preparative-scale operation emerges from such behavior. Sample loading may take place at pH 4.5 where the anti-Langmuir isotherm leads to a relatively increased amount of adsorption with increased protein solution concentration. Desorption could then take place at pH 6.0 where the protein would presumably be dissociated and only a single species (dimer) would elute for a sharper band profile than if two species were present (*i.e.*, dimer and tetramer) (see Fig. 4). Clearly, full reversibility with change in pH is required for this strategy to be successful.

ACKNOWLEDGEMENTS

The authors gratefully acknowledge the support of this work by NIH under GM-15847 and by Merck, Sharp & Dohme Research Laboratories. They also thank R. Mhatre for assistance in the LALLS measurement of the molecular weight. This is contribution No. 461 from the Barnett Institute.

REFERENCES

1 J. D. Andrade, in J. D. Andrade (Editor), *Surface and Interfacial Aspects of Biomedical Polymers*, Vol. 2, Plenum Press, New York, 1985, p. 1.
2 T. A. Horbett and J. L. Brash, in J. L. Brash and T. A. Horbett (Editors), *Proteins at Interfaces: Physicochemical Aspects and Biomedical Studies*, American Chemical Society, Washington, DC, 1987, p. 1.
3 J. M. Jacobson, J. H. Frenz and Cs. Horváth, *Ind. Eng. Chem. Res.*, 26 (1987) 43.
4 G. Guiochon and A. Katti, *Chromatographia*, 24 (1987) 165.
5 N. Grinberg, R. Blanco, D. M. Yarmush and B. L. Karger, *Anal. Chem.*, 61 (1989) 514.
6 R. Blanco, A. Arai, N. Grinberg, D. M. Yarmush and B. L. Karger, *J. Chromatogr.*, 482 (1989) 1.
7 H. A. McKenzie, in H. A. McKenzie (Editor), *Milk Proteins: Chemistry and Molecular Biology*, Vol. II, Academic Press, New York, 1970, p. 304.

8 T. F. Kumosinski and S. N. Timasheff, *J. Am. Chem. Soc.*, 88 (1966) 5635.
9 H. P. Jennissen, in J. L. Brash and T. A. Horbett (Editor), *Proteins at Interfaces: Physicochemical Aspects and Biomedical Studies*, American Chemical Society, Washington, DC, 1987, p. 295.
10 H. P. Jennissen, in I. M. Chaiken, M. Wilchek and I. Parikh (Editors), *Affinity Chromatography and Biological Recognition*, Academic Press, New York, 1983, p. 281.
11 H. P. Jennissen and G. Botzet, *Int. J. Biol. Macromol.*, 1 (1979) 171.
12 J.-X. Huang, J. Schudel and G. Guiochon, *J. Chromatogr.*, 504 (1990) 335.
13 S.-L. Wu, K. Benedek and B. L. Karger, *J. Chromatogr.*, 359 (1986) 3.
14 N. T. Miller, B. Feibush and B. L. Karger, *J. Chromatogr.*, 316 (1984) 519.
15 F. Riedo and E. Kováts, *J. Chromatogr.*, 239 (1982) 1.
16 J. Jacobson, J. Frenz and Cs. Horváth, *J. Chromatogr.*, 316 (1984) 53.
17 R. Mhate, I. S. Krull and H. H. Stuting, *J. Chromatogr.*, 502 (1990) 21.
18 L. Lapidus and A. R. Amundson, *J. Phys. Chem.*, 56 (1952) 984.
19 S. Golshan-Shirazi and G. Guiochon, *J. Chromatogr.*, 506 (1990) 495.
20 T. T. Herskovits, R. Townend and S. N. Timasheff, *J. Am. Chem. Soc.*, 86 (1964) 4445.
21 S. N. Timasheff and R. Townend, *Nature (London)*, 203 (1964) 517.